University of Baghdad
College of Engineering
JE
JOURNAL OF ENGINEERING

Journal of Engineering

journal homepage: www.jcoeng.edu.iq

Volume 30 Number 12 December 2024

Effects of Preparation Conditions on Performance of PES:PEG Flat Sheet Membrane for MG Dye Separation

Ihal A. Abed, **Basma I. Hussein***

Department of Chemical Engineering, College of Engineering, University of Baghdad, Baghdad, Iraq

Abstract

This study deals with the morphology and performance properties of a novel thin flat sheet ultrafiltration membrane; Malachite Green (MG) dye filtration behavior was evaluated in the cross-flow filtration system. The prepared membranes included the incorporation of 16 wt. % of polyether sulfone (PES)/DMF and 5 wt.% of Polyethylene Glycol (PEG) via the phase inversion process. Adding PEG decreased the internal concentration polarization, improved the membrane hydrophilicity, changed pore morphologies, and enhanced membrane performance. The SEM and AFM tests were used to characterize the composition and structure of the membrane. With different casting conditions, the membrane shape changed. The effect of membrane thickness (100, 150, and 200) µm and coagulation bath properties temperature (15, 25, and 35) °C and composition DMF (10, 20, 30 %) in water on the fabricated membrane were investigated. To evaluate the membrane filtration performance, the fabricated membranes were applied in an ultrafiltration system to treat Malachite Green dye solution at a concentration of (10 ppm) as a model pollutant. Based on the obtained results, the ideal membrane parameters were150 µm in thickness, 35°C in temperature, and 10% in composition DMF; the removal efficiency was observed to be (94.5%, 93%, and 99.5%) while the permeate flux (45, 35 and 30) LMH, respectively.

Keywords: Composite UF membrane, Membrane characterization, Malachite Green Dye separation, Phase inversion process, Permeate flux.

1. INTRODUCTION

Industrial wastewater pollution consists of multiple organic and inorganic pollutants, including dyes, which must be treated before being discharged into the environment. However, effluents are discharged from various sectors, including textile, wool, leather, silk, paper, pulp, ink, cosmetics, pharmaceuticals, and the food industry **(Mahmood and Waisi, 2021; Al-Bayati et al., 2023)**. It is important to know the content of wastewater before releasing it into water systems (such as lakes and rivers) or land to choose the most

*Corresponding author
Peer review under the responsibility of University of Baghdad.
https://doi.org/10.31026/j.eng.2024.12.12

Article received: 03/05/2024
Article revised: 14/06/2024
Article accepted: 23/06/2024
Article published: 01/12/2024

appropriate treatment method **(Hussein, 2010; Fadhil and Eisa, 2019)**. Even small concentrations of dyes in bodies of water can significantly reduce their attractiveness and visual appeal. In this context, color concentrations as low as 1 ppm may dramatically alter the perception of a specific color **(Waisi et al., 2015; Shayesteh et al., 2016)**. It also causes the water to become turbid and the gas ranges to drop. Hence, it is necessary to detect a feasible wastewater treatment strategy to avoid the coloration of textile industry effluent **(Mohammed et al., 2020; Mohammed *et al.*, 2023)**. Recently, there have been many changes in the advancement of membrane separation techniques. The membrane technology is significant in ensuring water and energy sustainability due to its remarkable effectiveness and safety **(Alkarbouly and Waisi, 2022a)**. Membrane processes use a barrier to separate elements from water and can extract components, such as dissolved organic and inorganic ions, dissolved solids, and heavy metals. Processes performed on various membrane surfaces, including reverse osmosis (RO), ultrafiltration (UF), microfiltration (MF), as well as nanofiltration (NF), which is often used in wastewater treatment. The UF and NF filtration membrane processes are common water purification strategies and are used to treat water to make it potable and highly purified, and also used in chemical process separations and seawater desalination **(Mustafa and Nakib, 2013; Akaood et al., 2024)**. Membrane filtration methods using UF usually mechanically separate substances from the mixture **(Al Aani et al., 2020)**.

It should be noted that polymeric membranes may lead to cost benefits. However, their structural asymmetry inevitably affects surface porosity and permeability **(Alkarbouly and Waisi, 2022b)**. This polymer is one example alongside the commercial polyethersulfone (PES) family. It has valuable working functions because it has superior mechanical and thermal stability, outstandingly good thermal aging performance, and outstanding environmental resistance. Moreover, PES shows some beneficial properties, which are relevant for processing purposes **(Safarpour et al., 2016; Abed and Waisi, 2024a)**. Previous research works have discussed several aspects to improve upon the performance of the membrane structure and the separation-related properties including the creation of an active layer (AL) using various weight percent (0-0.012 weight percent) of graphene oxide (GO), 1, 3-phenylenediamine and 1, 3, 5- Benzene trichloride into polyam. The introduction of PEG 400, PS, and 1-methyl, 2-pyrrolidone at various concentrations (0-8 wt. %) through the solvent evaporation process. The contact angles of the TFN-FO membranes experimentally witnessed increased hydrophilicity, porosity, water permeability, and water flow in comparison with the traditional TFC membranes **(Saeedi-Jurkuyeh *et al.*, 2020)**. Besides, the type of polymer and its properties for making membranes are crucial ones for membrane fabrication, and the use of solvents in the manufacturing of the membrane also plays a significant role in the preparation of casting solution. It is essential to choose a solvent with high purity and negligible water content, where it was prepared membranes of PPSU by immersion precipitation in DMA, NMP, and a mixture of DMF: NMP (50/50wt.%). Whilst macrovoids might cause unintended mechanical failures in the high-pressure application; therefore, proper control over macrovoid formation is crucial **(Darvishmanesh *et al.*, 2011)**. Thus, the effects of various parameters as the membrane thickness, bath temperature, and bath solvent contributions, are considered in the control of layer set formation **(Conesa et al., 2007)**.

This research applied a modified Polyether sulfone (PES) membrane with a phase inversion technique to fabricate a two-layer tubular composite ultrafiltration (UF) membrane which showed promising results. The impacts of composite UF membranes on cross-sectional morphology, hydrophilicity, roughness, permeate flux, and Malachite Green dye removal

efficiency were proposed. SEM, AFM, and porosity analysis were used to determine the final UF membrane microstructure.

2. MATERIALS AND METHOD

2.1 Materials

Polyether sulfone (PES) with 56,000 g/mol molecular weight was supplied by Basf, a US-based company. The polyethylene glycol (PEG) with a molecular weight of 6,000 g/mol was manufactured by Himedia Laboratories Pvt. Ltd, India. These polymers have been used to prepare the precursor solutions. The N,N-Dimethylformamide solvent (DMF, $HCON(CH_3)_2$, minimum assay 99%) was purchased from Amber Nath, India. The Chemical ($C_{23}H_{26}N_2Cl$), Malachite green dye (MG) was ordered from Sigma-Aldrich, USA.

2.2 The Flat Sheet Membrane Preparation

A thin film PES: The PEG-based membrane was made from the phase inversion technique. The existing casting precursor was a blend of 16 wt. 5 % of PES/DMF and 5% of PEG/DMF. Within the membrane, polyethylene glycol would drop the internal concentration polarization, and therefore improve membrane performance by increasing membrane hydrophilicity and transforming pore structures. The casting solution was formed by mixing the PEG with the DMF solvent with a magnetic stirrer for 6 h, and then the PES was added and magnetically stirred for 6 h. The casting solution was allowed to be degassed for 24 hours. Then, the casting precursor solution was applied at a certain thickness on a clean glass plate using a casting Gardner knife (Filmography: film casting doctor blade). The glass plate with the casted polymeric film was carefully submerged in the coagulation bath. After a while, the phase inversion occurred, and a solid thin film layer membrane floated off the glass surface. The prepared membranes should be stored in the DI water bath for at least 24 h to get rid of all the access solvents and dissolve the PEG polymer, creating the required pores with the membrane.

The impact of the coagulation bath properties (temperature and composition) on the PES:PEG membrane properties was investigated. The prepared membranes were immersed in the coagulation bath at different temperatures (15, 25, and 35) °C$\pm$1°C. Also, different percentages of DMF (10, 20, and 30%) were mixed with the water bath to investigate its effect on the morphology and surface characterization of the prepared membrane. Besides that, the impact of membrane thickness was studied by preparing membranes of different thicknesses (100, 150, and 200) μm, as shown in **Table 1.**

Table 1. The composition of ultrafiltration membranes and fabrication conditions

Membrane thickness (μm)	Temperature (°C)	DMF in water bath (%)
150	35 25 15	0
100 150 200	35	0
150	35	10 20 30

2.3 Characterization Methods

The scanning probe microscopy (SPM AA300 Angstrom Advanced Inc., AFM, USA) was applied to analyze the roughness surface to clarify the nature of the ultrafiltration membrane. The membranes were prepared before being cut into tiny squares and bonded to a metal supporting body. One micron by one micron was applied to photomicrograph the plasmalemma. The membrane was scanned in the tapping mode, and all heat measurements were made on artificial membranes dried with natural atmospheric conditions. A so-called scanning electron microscope (SEM) was used in connection with a TESCAN VEGA3 SB instrument, EO Electronic-Optic-Service GmbH, Germany to observe the surface morphology and cross-section of the films. Before the SEM observation, membranes were cracked, sputtered with platinum, and frozen in liquid nitrogen as samples. Following that, SEM inspections with a potential of 5.00 kV at various magnifications were performed on the dried sample of membranes. Characterizing membrane porosity is important in various membrane applications, particularly concerning membrane separation performance **(Al-Okaidy and Waisi, 2023).**

Each membrane sample was taken, and then the weighing process was completed in order to evaluate the flat sheet membranes with respect to their porosity. The samples were next offered the chance to be immersed in distilled water for the time of two minutes. The sample's dry and wet weights were measured and recorded right after distill water immersion by weighing the sample. The flat sheet membrane porosity was measured gravimetrically and was used in the calculation to get the overall porosity, which is represented by Eq.(1) **(Sabeeh and Waisi, 2022).**

$$\varepsilon = \frac{M_1 - M_2}{A * l * d} * 100 \quad (1)$$

where ε is the overall porosity, M_1 is the wet membrane weight (g/m^3), M_2 is the dry membrane weight (g/m^3), A is the membrane effective area (m^2), l is the membrane thickness (m) and d is the water density (998 kg/m^3 at 25 °C). The results of three independent replications of each test were considered.

2.4 Membrane Performance Test

All the fabricated membranes were tested for dye separation using a cross-flow filtration system. The system comprised a cross-flow filtering cell, feed pump, feed solution tank, and pressure gauge. The constructed membrane was cut into dimensions of 4 x 6 cm and secured in the membrane cross-flow cell, which had a filtration area of 24 cm^2. More details about the used system are illustrated in our previous work **(Abed and Waisi, 2024)**. The filtration system was initially run with distilled water for 15 minutes to stabilize the membrane's flow. The dye solution was used instead of water for filtration across the membrane. The performance of the ultrafiltration membranes was assessed based on pure water flow and dye removal. The permeability and removal of dye via the membrane were examined at room temperature and transmembrane pressures (6 bar) **(Wang et al., 2019)**. Eq. (2) was used to compute the permeate flux **(Salahi et al., 2010).**

$$F = \frac{V}{A \times t} \quad (2)$$

where F is the flux rate (L/m^2 h), V is the volume of permeate (L), A is the effective area (m^2), and t is the filtration time (h).
The solute rejection R (%) was calculated using Eq.(3) **(Mukherjee and De, 2014).**

$$R = \frac{Cf - Cp}{Cf} \times 100 \quad (3)$$

Where R represent the rejection (%). The Cf and Cp represent the concentrations (mg/L) in the feed and permeate solutions, respectively. An ultraviolet-visible spectrophotometer was used to calculate the dye's concentration.

3. RESULTS AND DISCUSSION

3.1 Membrane Characterization

Fig. 1 depicts the surface and cross-sectional scanning electron microscopy (SEM) images of the composite membranes containing 16wt.% Polyethersulfone (PES):5wt.% Polyethylene glycol (PEG) at different parameters. The thickness of the membrane plays an important role during the structure development. **Fig. 1 (A, B, and C)** shows SEM images of the cross and surface structure morphology for composite PES:PEG membranes with various thicknesses: (A)100 µm, (B)150 µm, and (C)200 µm. Reducing the thickness of the membrane improves the internal macro void dimensions. The mechanism of macro void creation during membrane precipitation explains the phenomenon. Macrovoid initiation often occurs at the membrane surface with a low polymer concentration and they develop far away from the skin as the thickness of the membrane is increased. In other words, the size of macro voids can be limited by increasing the thickness of the casting solution from 100 µm to 150 µm and 200 µm **(Vogrin et al., 2002).**
Changes in the coagulation bath temperature affect the system's thermodynamic and kinetic parameters, affecting the conditions and results of the phase inversion process. **Fig. 2 (A, B, and C)** shows SEM images of the surface and cross-structure morphology for composite membranes at different coagulation temperatures: (A) 15 °C, (B) 25 °C, and (C) 35 °C. The cross-sectional SEM pictures of the membrane obtained at 15 °C in **Fig. 2A** show an asymmetric structure with a spongy sublayer. When comparing the cross-sectional SEM pictures of the skin regions of the membranes made at 15 °C contain a more dense skin layer. Increasing the temperature to 25°C and 35°C grows the surface pores of the membrane and changes the membrane sublayer structure from spongy to finely developed pores. Microvoids form faster at higher temperatures (Mohammadi and Saljoughi, 2009). Through the slow demixing, nucleation occurs after some time, leading to a rise in polymer concentration in the top layer of the membrane. Nucleation begins in the lower layer at short and successive time intervals. Therefore, the size and content of nuclei in the former layer are such that new nuclei gradually form in their neighborhood. Slow demixing prevents the unrestricted growth of limited nuclei on the top layer. As a result, large voids are prevented, and denser membranes are produced instead of fast separation **(Amirilargani et al., 2010).**
Adding organic solvent (such as DMF) to the coagulation bath is considered a characteristic effect on the surface layer's shape and the membrane's morphology and performance. **Fig. 3 (A, B, and C**) displays the SEM of the surface and cross membranes treated with different concentrations of DMF (10, 20, and 30) wt.% in the coagulating bath, and 150 µm of

membrane thickness was kept constant. The solubility properties of the solvent and nonsolvent are physical parameters that influence the membrane structure **(Madaeni and Taheri, 2011).**

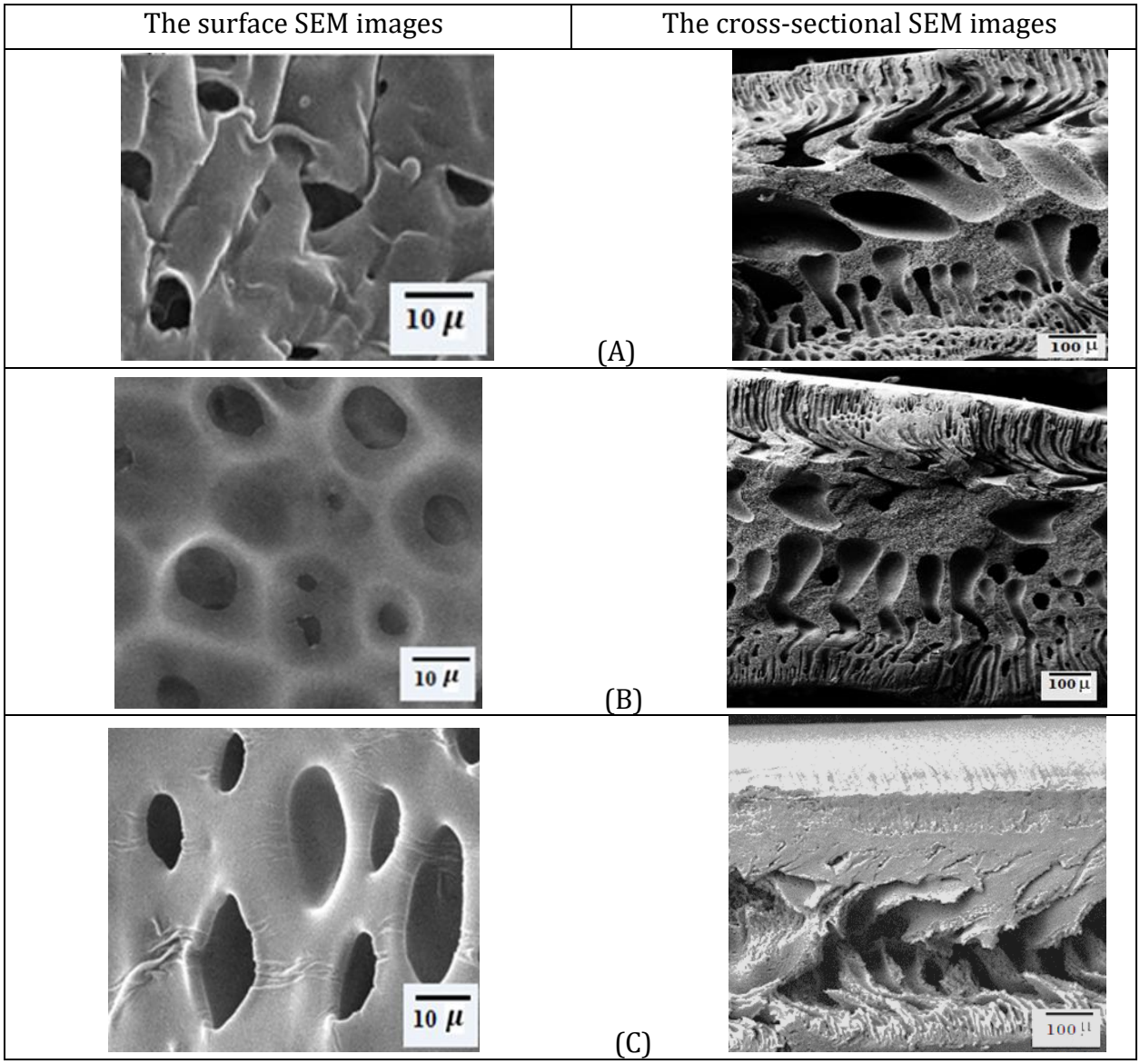

Figure 1. The SEM images of the surface and cross-structure morphology of A (100 μm), B (150 μm), and C (200 μm) composite UF membranes.

When the solvent and nonsolvent have significantly different solubility parameters, the nonsolvent can diffuse the polymer layer more easily, resulting in an increased exchange rate between the solvent in the polymer film and the nonsolvent in the coagulation bath. This leads to immediate separation, typically including a porous surface layer and the creation of finger-shaped pores in the underlying layer. On the other hand, delayed demixing, resulting from minimal changes in solubility parameters between the solvent and nonsolvent, is frequently linked to creating a dense layer. The membrane formed in 10 % DMF and pure water in **Fig. 3A** displayed a symmetrical structure without a dense top layer. The membrane has a porous structure across its entire cross-section.

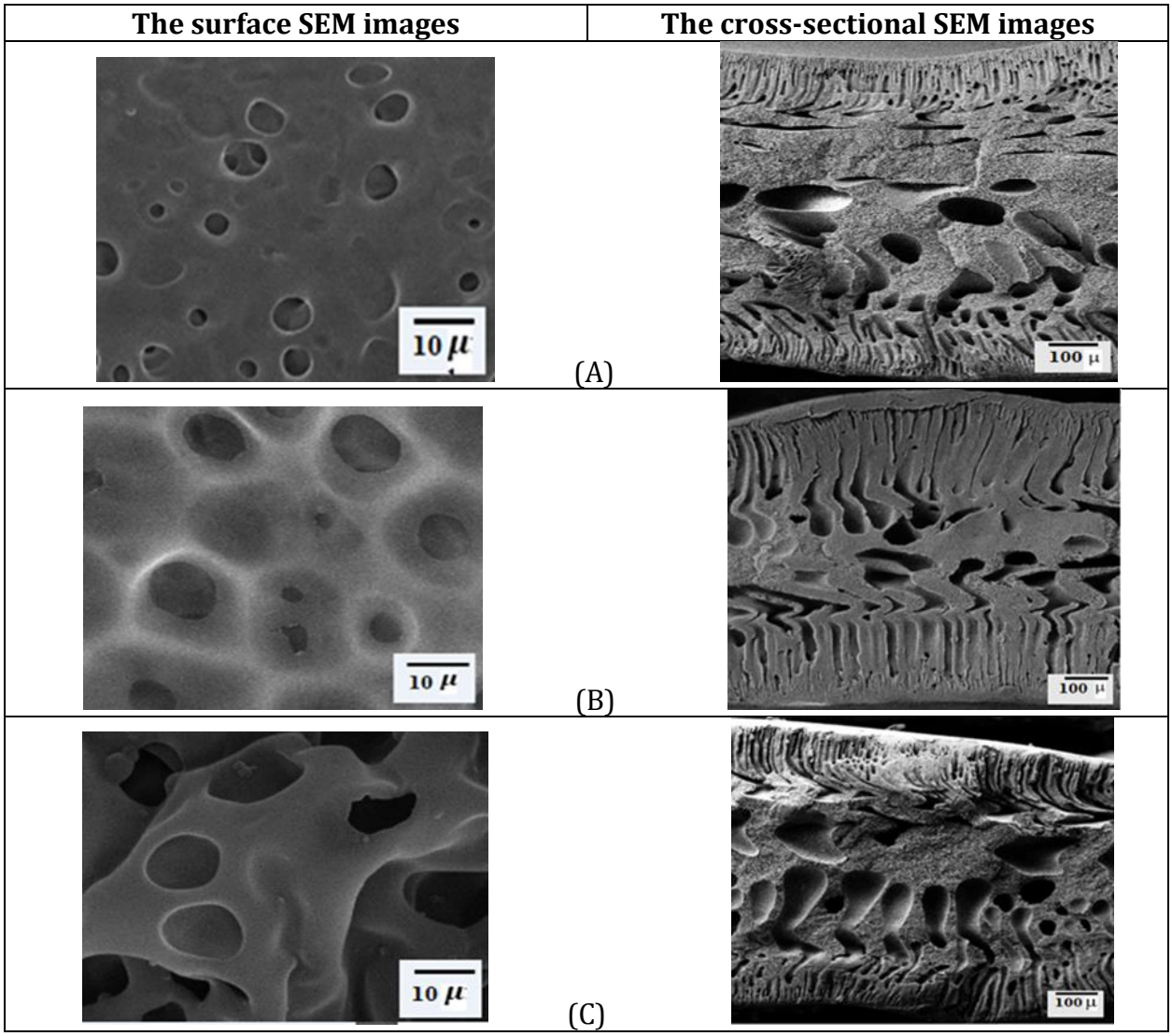

Figure 2. The SEM images of the surface and cross-structure morphology of A (15°C), B(25°C), and C(35°C) composite UF membranes.

The cavities are separated by walls made of distinct polymer globules. The porous sublayer structure is distributed uniformly through the membrane's cross-section. The pore size of the outer surface increased as the DMF content rose. Coagulation plays an important role in the creation of membranes by phase inversion methods, and the coagulation process weakens as the ratio of DMF increases to (20% and 30%) in the bath. It leads to a porous structure, like a sponge **(Madaeni and Taheri, 2011).** Adding a hydrophilic PEG particle to the PES dope solution leads to a notable increase in the exchange rate between the solvent and non-solvent compared to the pristine version. This is evidenced by the accelerated diffusion of water into the as-cast polymeric film. Subsequently, assuming a prominent role in initiating macro void formation and overall porosity enhancement **(Razmjou et al., 2011).**

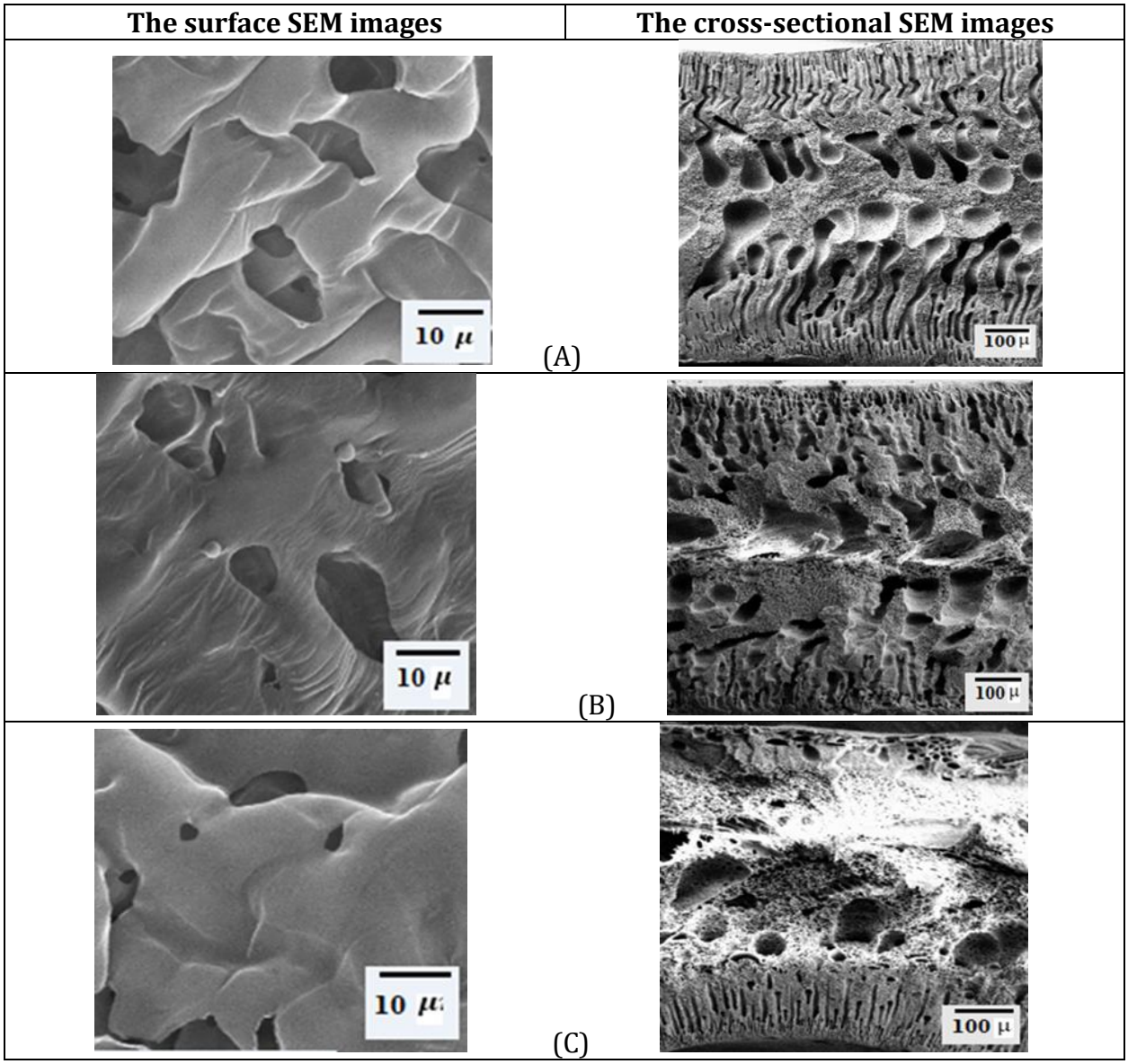

Figure 3. The SEM images of the surface and cross-structure morphology of A(10%DMF), B(20%DMF), and C (30%DMF) composite UF membranes.

The SEM and AFM results showed a significant correlation between membrane thickness and affects both surface roughness **(Güzelçimen *et al.*, 2020)**. **Figs. 4 to 6** display three-dimensional AFM pictures of composite membranes' top surfaces made at various parameters with scan sizes of 10 μm×10 μm. **Fig. 4 (A, B, and C)** displays AFM pictures of various Thickness (100,150, and 200) μm. The presence of change in the membranes' thickness changes the membranes' surface morphology. Many factors can alter the surface properties, including chain wrinkling development, electrostatic interactions between polymer chains, density or bending, and variations in the surface area **(Esmaeili, 2010)**. The little peaks and valleys were replaced by several large ones when the thickness was increased, resulting in a rough membrane surface. The membrane with 200 μm indicated higher roughness (83.53 nm) than the membrane of 150 μm (81.65 nm) and 100 μm (40.94 nm). Surface roughness is an important characteristic and effect of coagulant temperature. **Fig. 5 A, B, and C** display AFM pictures of various coagulant temperatures (15,25 and 35) °C.

So, at a coagulant temperature of 15°C, the roughness was 17.85 nm. And when the coagulant temperature was raised to 25°C and 35°C, the roughness increased to 40.38 nm and 81.65 nm, respectively. Increasing the coagulant temperature speeds up the interaction between the new membranes' solvent and the coagulation bath's non-solvent. This leads to increased roughness and more significant depressions on the membrane surface, which is a sign that the size of the surface pore is growing **(Amirilargani et al., 2015).**

The change in roughness may be caused by variations in the added solvent (DMF) ratio in the coagulation bath. **Fig. 6A, B, and C** display AFM pictures of various coagulant solvent (DMF) ratios (10,20 and 30) wt.%. The membrane prepared using 10% DMF as a coagulation bath had a roughness of 24.46 nm, lower than those prepared with DMF at 20% and 30%, which had a roughness of 24.63 nm and 56.26nm, respectively. This difference is due to the slower diffusion rate in 10% DMF compared to 20% and 30% DMF. It might be considered that the DMF membrane with a smaller ratio had denser skins and finer surfaces. It is widely known that smoother surfaces increase a membrane's resistance to fouling. The slight roughness difference is due to considering the overall membrane structure, not just the top layer **(Al-Furaiji et al., 2022)**. Less rough 10% DMF membranes had a lower flow reduction coefficient for this reason.

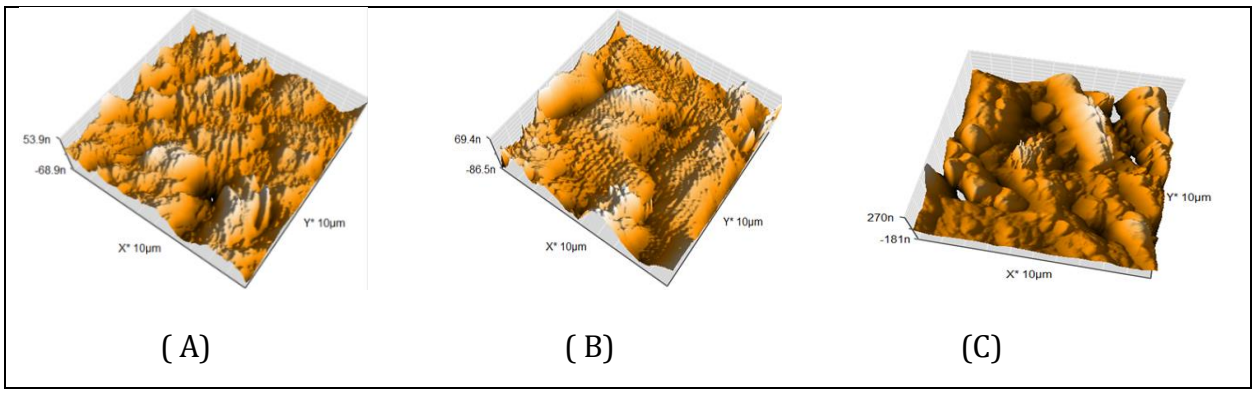

Figure 4. The AFM images of the A (100 µm), B (150 µm), and C (200 µm) composite UF membranes

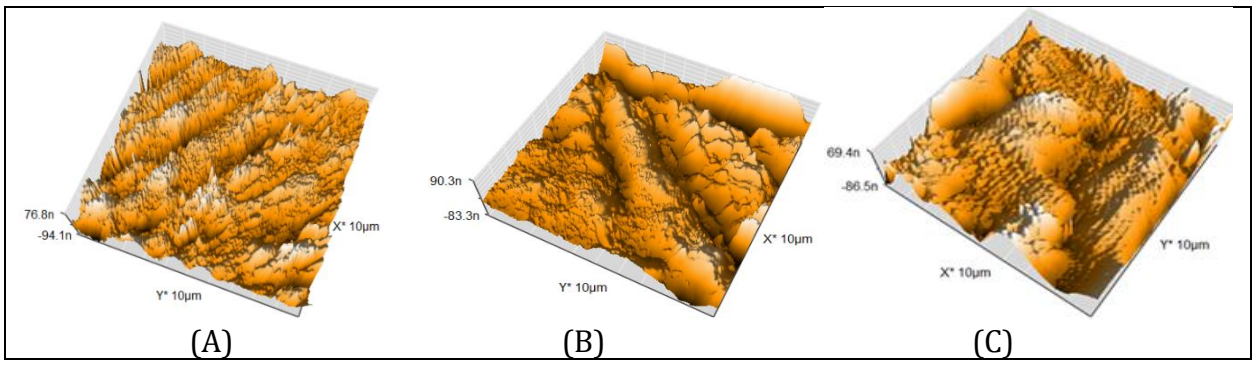

Figure 5. The AFM images of the A (15 °C), B (25 °C), and C (35 °C) composite UF membranes

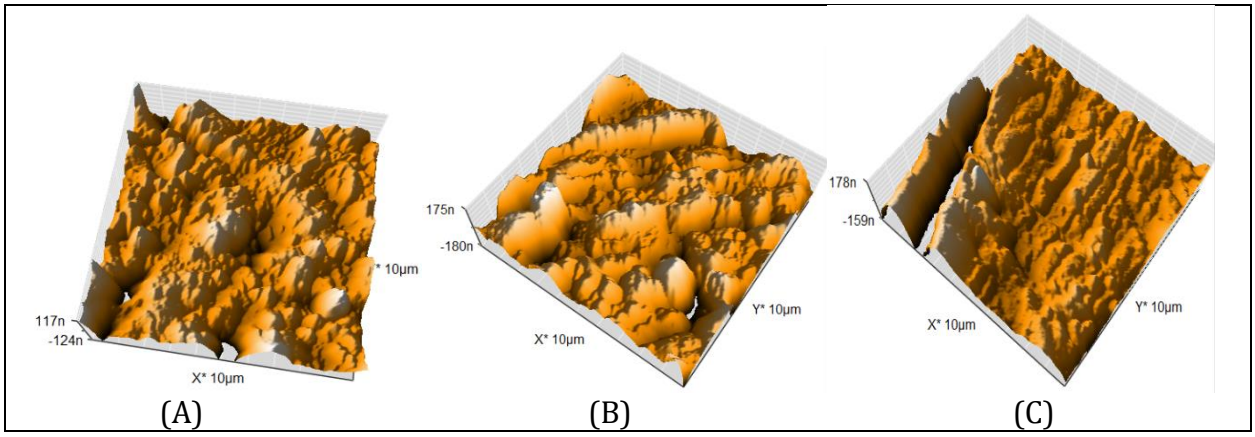

Figure 6. The AFM images of the A (10wt.%), B (20wt.%), and C (30wt.%) composite UF membranes

Table 2 examines the top surfaces of the PES:PEG membranes across a 4 cm^2 region to determine their porosity and average roughness (Ra), representing the surface's average deviation from the center plane. An observable correlation occurs between the high temperature and ratio of DMF when membrane fabrication that an increase in membrane porosity when demonstrated. In addition, the membranes showed porosity affected by manufacturing conditions.

Table 2. Obtained parameters of coil roughness and porosity of the prepared films

PES:PEG Membrane	Porosity (%)	Average Roughness, Ra (nm)
Temperature (°C)		
15	31	17.85
25	33.3	40.38
35	35.3	81.65
DMF in water bath (%)		
10%	36.5	24.46
20%	38.4	24.63
30%	38.9	56.26
Thickness (µm)		
100	37	40.94
150	35.3	81.65
200	34.9	83.53

Table 2 presents the surface roughness measurements. The surfaces of fabrication membranes were discovered to possess a somewhat more uneven texture. The increased surface roughness may be attributed to the ratio of DMF in bath water on the surface. Numerous studies have extensively documented this behavior, as indicated by references **(Ahmad *et al.*, 2017; Kakar et al., 2015).**

3.2 Membrane Performance Test

The development of membrane fouling substantially impacts the efficiency and longevity of membrane filtering systems in terms of fluid separations and operational lifespan. The

reduction in membrane flux can be attributed to many factors, such as the obstruction or occlusion of membrane pores, concentration polarisation, and the creation of cake layers. A high-quality membrane should have high flux, low fouling tendency, and a sustained high rejection rate. The occurrence of membrane fouling can be attributed to various underlying factors. The key factor contributing to the suboptimal antifouling performance of membranes is the hydrophobic nature of their surfaces **(Koo et al., 2012**). Several strategies have been employed to improve the hydrophilicity of membranes, such as material modification, polymer mixing, and surface modification **(Kumar *et al.*, 2013).**

Fig. 7 (A and B) show the effect of membrane thickness on flux and rejection, respectively. The data revealed that dye removal increased as the thickness of the membrane Increased, as it started at 90.5% when the thickness was (100 µm) and continued to rise steadily at (94.5% and 95%) at the thickness increased to (150 and 200) µm, respectively. In contrast, the water flux decreased, as it started at 60 LMH in the thickness of the membrane (100 µ m), and it continued to decrease from (45 to 35) LMH at the thickness of the membrane (150 and 200) µm, respectively **(Güzelçimen et al., 2020; Cui et al., 2010).**

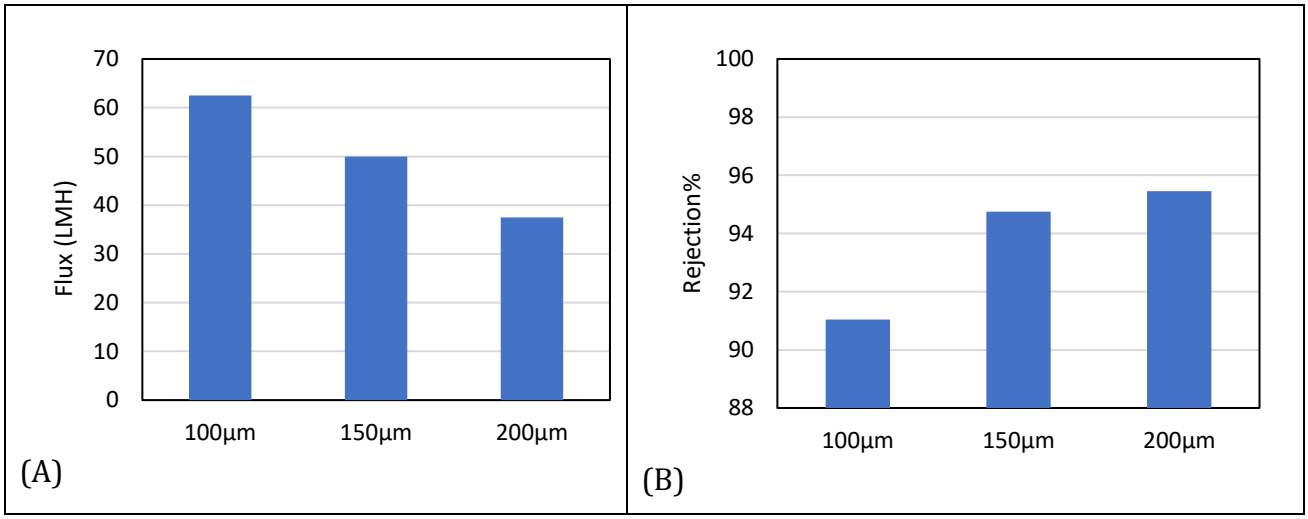

Figure 7. (A) water flux and (B) Rejection of dye versus thickness of the membrane (100,150 and 200) µm, at16% PES/5%PEG membranes

Fig. 8 (A and B) represents the pure water flux and dye rejection towards different bath temperatures (15, 25, and 35) °C for the membranes, respectively. A decrease in temperature, 15°C was a strong enough resistance for the membrane to prevent the water from passing through because it has a small pores volume that results in low mutual diffusivities between the system components when the casting solution is solidified. This delays precipitation, leading to a thick membrane and higher polymer concentration in both the top layer and sublayer **(Güzelçimen et al., 2020),** and increasing bath temperatures from 15˚C to 25˚C results in a rise in pure water flux from 0 to 35 LMH. The membrane created at bath temperatures of 15°C and 25°C had dye rejection rates of 0% and 93%, respectively. As the bath temperatures rise from 25°C to 35°C, the permeation flux increases to 45 LMH, while the dye rejection reduces to 90%. The pure water flux is directly associated to the porosity of the top layer of the membrane **(Madaeni and Taheri, 2011).** Decreasing bath temperatures significantly decreases membrane porosity, resulting in a denser structure in both the upper layer and the sublayer **(Razmjou et al., 2011).**

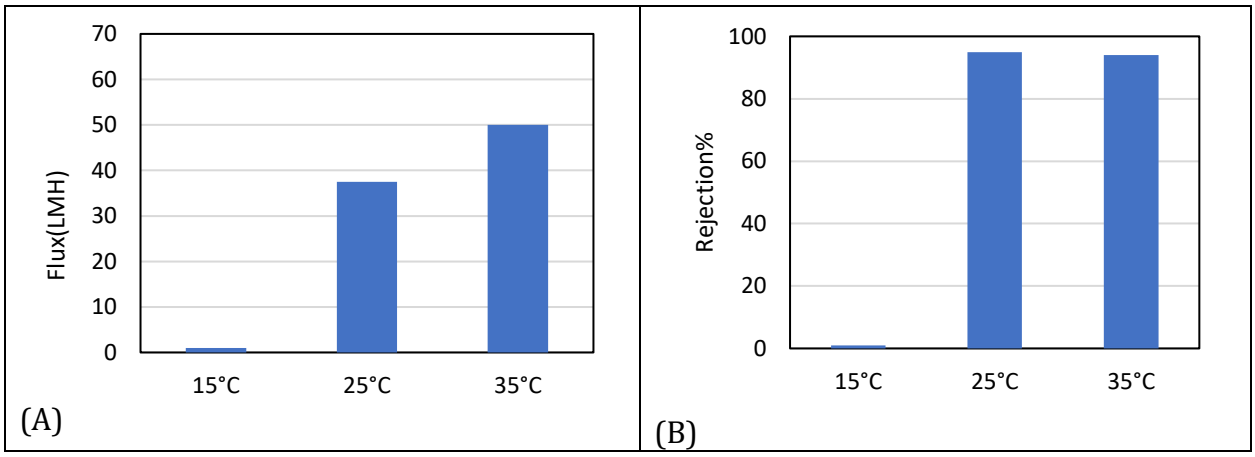

Figure 8. (A) water flux and (B) Rejection of dye different bath temperatures (15, 25, and 35) °C.

Permeability has a direct connection to pore creation from the coagulation bath. **Fig. 9 (A and B**) shows the changes in pure water flux and rejection, respectively. When dye is present in composite ultrafiltration membranes with varying ratios of DMF (0,10, 20, and 30) wt. %. The flux of solutions containing 0 wt.% DMF, 10wt.% DMF and 20wt.% DMF are 50 LMH, 30 LMH and 32 LMH, respectively. The rejection rates were 0 wt.%, 10wt.% and 20wt.% for 94%, 99.5% and 99.63%, respectively. The permeate flux of 30wt.% DMF is 42.5 LMH, with a rejection rate of around 93.7%. The flux increased, and rejection decreased gradually as the pore size and porosity increased **(Luo *et al.*, 2009).**

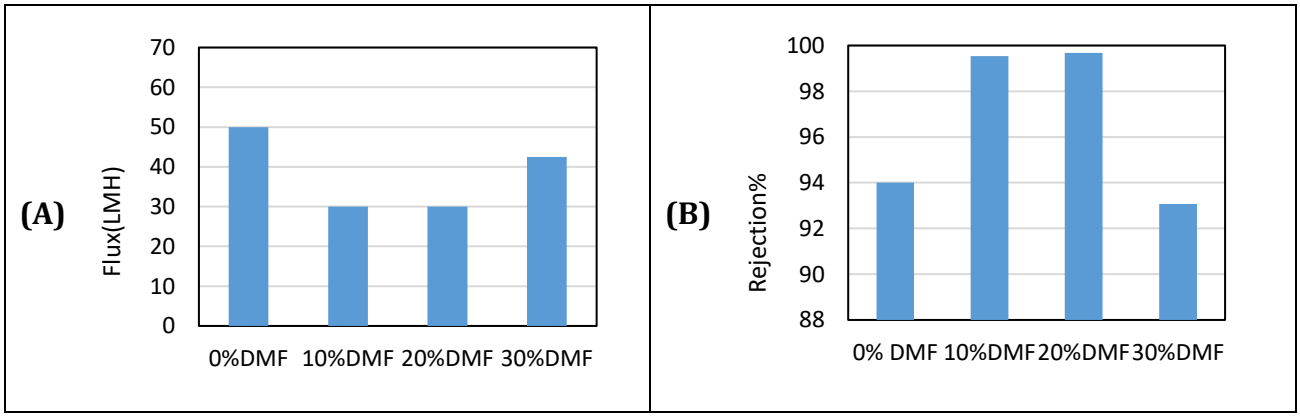

Figure 9. (A) water flux and (B) Rejection of dye different bath DMF (0,10, 20 and 30 %)

4 . CONCLUSION

The membrane which was produced by the phase inversion method is subjected to the subsequent tests to remove MG dye. The solution of PES: PEG was taken as a membrane which forms the ultrafiltration mode. The selected parameters, such as the thickness of the membrane, the effect of temperature, and DMF in the water bath, were to evaluate its ability to remove the dye. The SEM images found important changes in the membrane morphology and increased the surface porosity of the composite membranes, with high temperature

and DMF concentration as the increasing agent and membrane thickness as the cutting factor. AFM imaging reveals that the membrane surface roughness of the composite is a function of dimensions of parameter variation. The rejection increased with the rise in temperature and thickness and decreased with the concentration of DMF in the water bath membranes. The optimum condition was (temperature=25°C, thickness=150 µm, and DMF ratio=10 %) for removing MG dye. The Malachite Green dyes at 10 ppm and 6 bar concentrations for all the membranes studied.

NOMENCLATURE

Symbol	Description	Symbol	Description
A	The membrane effective area (m^2)	M_1	The wet membrane weight(g/m^3)
Cf	The dye concentration in the feed (mg/L)	M_2	The dry membrane weight (g/m^3)
Cp	The dye concentration in the permeate (mg/L)	*R*	The dye rejection (%)
d	The water density (g/cm^3)	t	Filtration time (h)
F	Flux rate (L/m^2 h)	V	The volume of permeate (L)
l	The membrane thickness (m)	ε	The porosity

Acknowledgments

The authors would like to thank the Department of Chemical Engineering- University of Baghdad for the support in performing the experimental work and the required analysis.

Credit Authorship Contribution Statement

Ihal Ali: Writing the draft version, methodology, and experimental work.
Basma Ismael: Reviewing, data analysis, proofreading, and supervision.

Declaration of Competing Interest

The authors declare that they have no known competing financial interests or personal relationships that could have appeared to influence the work reported in this paper.

REFERENCE

Abed, I.A. and Waisi, B.I., 2024a. Performance enhancement of Polyethersulfone-Based Ultrafiltration Membrane Decorated by Titanium Dioxide Nanoparticles for Dye Filtration, *Ecological Engineering & Environmental Technology*, 25(5), pp. 265–273. https://doi.org/10.12912/27197050/186182

Abed, I.A. and Waisi, B.I., 2024b. Preparation and characterization of PES flat sheet membrane embedded with PEG for dye filtration application. *Iraqi Journal of Applied Physics*, 20(2A), pp.179-186.

Ahmad, A.L., Abdulkarim, A.A., Shafie, Z.M. and Ooi, B.S., 2017. Fouling evaluation of PES/ZnO mixed matrix hollow fiber membrane. *Desalination*, *403*, pp. 53-63. https://doi.org/10.1016/j.desal.2016.10.008

Akaood, M.A., Ali, I.M. and Waisi, B.I., 2024. Water Treatment Performance of PAN/HPMC/Gr Nano Composites. *Iraqi Journal of Physics*, *22*(1), pp.42-52. https://doi.org/10.30723/ijp.v22i1.1175

Al Aani, S., Mustafa, T.N. and Hilal, N., 2020. Ultrafiltration membranes for wastewater and water process engineering: A comprehensive statistical review over the past decade, *Journal of Water Process Engineering*, 35, pp. 1–36. https://doi.org/10.1016/j.jwpe.2020.101241.

Al-Bayati, I.S., Abd Muslim Mohammed, S. and Al-Anssari, S., 2023. Recovery of Methyl Orange from Aqueous Solutions by Bulk Liquid Membrane Process Facilitated with Anionic Carrier, in *AIP Conference Proceedings,* (Vol. 2414, No. 1). American Institute of Physics Inc. https://doi.org/10.1063/5.0114631

Al-Furaiji, M., Waisi, B., Kalash, K. and Kadhom, M., 2022. Effect of polymer substrate on the performance of thin-film composite nanofiltration membranes. *International Journal of Polymer Analysis and Characterization*, *27*(5), pp.316-325. https://doi.org/10.1080/1023666X.2022.2073008.

Alkarbouly, S. and Waisi, B., 2022a. Dual-layer Antifouling Membrane of Electrospun PAN: PMMA Nonwoven Nanofibers for Oily Wastewater Treatment. In *Proceedings of 2nd International Multi-Disciplinary Conference Theme: Integrated Sciences and Technologies, IMDC-IST 2021, 7-9 September 2021, Sakarya, Turkey*. https://doi.org/10.4108/eai.7-9-2021.2314932.

Alkarbouly, S.M. and Waisi, B.I., 2022b. Fabrication of Electrospun Nanofibers Membrane for Emulsified Oil Removal from Oily Wastewater, *Baghdad Science Journal*, 19(6), pp. 1238–1248. https://dx.doi.org/10.21123/bsj.2022.6421

Al-Okaidy, H.S. and Waisi, B.I., 2023. The Effect of electrospinning parameters on morphological and mechanical properties of PAN-based Nanofibers Membrane, *Baghdad Science Journal*, 20(4), pp. 1433–1441. https://doi.org/10.21123/bsj.2023.7309.

Amirilargani, M., Sadrzadeh, M. and Mohammadi, T., 2010. Synthesis and characterization of polyethersulfone membranes. *Journal of polymer research*, *17*, pp.363-377. https://doi.org/10.1007/s10965-009-9323-6.

Conesa, A., Gumí, T. and Palet, C., 2007. Membrane thickness and preparation temperature as key parameters for controlling the macrovoid structure of chiral activated membranes (CAM). *Journal of Membrane Science*, 287(1), pp. 29–40. https://doi.org/10.1016/j.memsci.2006.10.006.

Cui, A., Liu, Z., Xiao, C. and Zhang, Y., 2010. Effect of micro-sized SiO2-particle on the performance of PVDF blend membranes via TIPS. *Journal of Membrane Science*, *360*(1-2), pp.259-264. https://doi.org/10.1016/j.memsci.2010.05.023

Darvishmanesh, S., Jansen, J.C., Tasselli, F., Tocci, E., Luis, P., Degrève, J., Drioli, E. and Van der Bruggen, B., 2011. Novel polyphenylsulfone membrane for potential use in solvent nanofiltration. *Journal of Membrane Science*, *379*(1-2), pp.60-68. https://doi.org/10.1016/j.memsci.2011.05.045.

Esmaeili, M., Madaeni, S.S. and Barzin, J., 2010. The dependence of morphology of solid polymer electrolyte membranes on transient salt type: effect of cation type, *Polymer International*, 59(7), pp. 1006–1013.

Güzelçimen, F., Tanören, B., Çetinkaya, Ç., Kaya, M.D., Efkere, H.İ., Özen, Y., Bingöl, D., Sirkeci, M., Kınacı, B., Ünlü, M.B. and Özçelik, S., 2020. The effect of thickness on surface structure of RF sputtered TiO_2 thin films by XPS, SEM/EDS, AFM and SAM. *Vacuum*, *182*, P.109766.

Fadhil, O.H. and Eisa, M.Y., 2019. Removal of methyl orange from aqueous solutions by adsorption using corn leaves as adsorbent material. *Journal of Engineering*, *25*(4), pp.55-69. https://doi.org/10.31026/j.eng.2019.04.05

Hussein, B.I., 2010. Removal of copper ions from wastewater by adsorption with modified and unmodified sunflower stalks. *Journal of Engineering,* 16(03), pp. 5411–5421. https://doi.org/10.31026/j.eng.2010.03.10

Kakar, M.R., Hamzah, M.O. and Valentin, J., 2015. A review on moisture damages of hot and warm mix asphalt and related investigations. *Journal of Cleaner Production*, 99, pp. 39–58. https://doi.org/10.1016/j.jclepro.2015.03.028

Kumar, R., Isloor, A.M., Ismail, A.F., Rashid, S.A. and Al Ahmed, A., 2013. Permeation, antifouling and desalination performance of TiO2 nanotube incorporated PSf/CS blend membranes. *Desalination*, *316*, pp.76-84. https://doi.org/10.1016/j.desal.2013.01.032

Luo, M.L., Wen, Q.Z., Liu, H.J. and Liu, J.L., 2009. Effect of TiO_2 nanoparticles on the hydrophilicity of sulfonated-polyethersulfone. *Advanced Materials Research*, *79*, pp.663-666. https://doi.org/10.4028/www.scientific.net/AMR.79-82.663.

Madaeni, S.S. and Taheri, A.H., 2011. Effect of casting solution on morphology and performance of PVDF microfiltration membranes. *Chemical Engineering & Technology*, *34*(8), pp.1328-1334. https://doi.org/10.1002/ceat.201000177.

Mahmood A., O. and Waisi, B.I., 2021. Synthesis and characterization of polyacrylonitrile based precursor beads for the removal of the dye malachite green from its aqueous solutions, *Desalination and Water Treatment*, 216, pp. 445–455. https://doi.org/10.5004/dwt.2021.26906.

Mohammadi, T. and Saljoughi, E., 2009. Effect of production conditions on morphology and permeability of asymmetric cellulose acetate membranes, *Desalination*, 243(1–3), pp. 1–7. https://doi.org/10.1016/j.desal.2008.04.010.

Mohammed, M.A., Al-Bayati, I.S., Alobaidy, A.A., Waisi, B.I. and Majeed, N., 2023. Investigation the efficiency of emulsion liquid membrane process for malachite green dye separation from water. Desalination and Water Treatment, 307, pp. 190-195. https://doi.org/10.5004/dwt.2023.29903

Mohammed, N.A., Alwared, A.I. and Salman, M.S., 2020. Photocatalytic Degradation of Reactive Yellow Dye in Wastewater using H_2O_2/TiO_2/UV Technique, *Iraqi Journal of Chemical and Petroleum Engineering*, 21(1), pp. 15–21. https://doi.org/10.31699/ijcpe.2020.1.3.

Mukherjee, R. and De, S., 2014. Adsorptive removal of phenolic compounds using cellulose acetate phthalate–alumina nanoparticle mixed matrix membrane. *Journal of hazardous materials*, *265*, pp.8-19. https://doi.org/10.1016/j.jhazmat.2013.11.012.

Mustafa, N. and Nakib, H.A.L., 2013. Reverse osmosis polyamide membrane for the removal of Blue and Yellow dye from waste water, I*raqi Journal of Chemical and Petroleum Engineering*, 14(2), pp. 49–55. https://doi.org/10.31699/IJCPE.2013.2.7

Razmjou, A., Mansouri, J. and Chen, V., 2011. The effects of mechanical and chemical modification of TiO_2 nanoparticles on the surface chemistry, structure and fouling performance of PES ultrafiltration membranes. *Journal of Membrane Science*, 378(1–2), pp. 73–84. https://doi.org/10.1016/j.memsci.2010.10.019

Sabeeh, H. and Waisi, B.I.W., 2022. Effect of Solvent Type on PAN–Based Nonwoven Nanofibers Membranes Characterizations, *Iraqi Journal of Chemical and Petroleum Engineering*, 23(4), pp. 43–48. https://doi.org/10.31699/ijcpe.2022.4.6.

Saeedi-Jurkuyeh, A., Jafari, A.J., Kalantary, R.R. and Esrafili, A., 2020. A novel synthetic thin-film nanocomposite forward osmosis membrane modified by graphene oxide and polyethylene glycol for heavy metals removal from aqueous solutions. *Reactive and Functional Polymers*, *146*, p.104397. https://doi.org/10.1016/j.reactfunctpolym.2019.104397.

Safarpour, M., Vatanpour, V. and Khataee, A., 2016. Preparation and characterization of graphene oxide/TiO2 blended PES nanofiltration membrane with improved antifouling and separation performance, *Desalination*, 393, pp. 65–78. https://doi.org/10.1016/j.desal.2015.07.003

Salahi, A., Abbasi, M. and Mohammadi, T., 2010. Permeate flux decline during UF of oily wastewater: Experimental and modeling. *Desalination*, *251*(1-3), pp.153-160. https://doi.org/10.1016/j.desal.2009.08.006.

Shayesteh, H., Rahbar-Kelishami, A. and Norouzbeigi, R., 2016. Adsorption of malachite green and crystal violet cationic dyes from aqueous solution using pumice stone as a low-cost adsorbent: kinetic, equilibrium, and thermodynamic studies. *Desalination and Water Treatment*, *57*(27), pp.12822-12831.. https://doi.org/10.1080/19443994.2015.1054315.

Vogrin, N., Stropnik, Č., Musil, V. and Brumen, M., 2002. The wet phase separation: the effect of cast solution thickness on the appearance of macrovoids in the membrane forming ternary cellulose acetate/acetone/water system. *Journal of Membrane Science*, *207*(1), pp.139-141. https://doi.org/10.1016/S0376-7388(02)00119-9

Waisi, B.I.H., Karim, U.F.A., Augustijn, D.C.M., Al-Furaiji, M.H.O., and Hulscher, S.J.M.H., 2015. A Study on the Quantities and Potential Use of Produced Water in Southern Iraq. *Water Science & Technology: Water Supply* 15 (2), P. 370. https://doi.org/10.2166/ws.2014.122

تأثيرات ظروف التحضير على أداء غشاء الصفيحة المسطحة المحضر من PES:PEG لفصل الصبغة الخضراء

ايهال علي عبد, بسمة إسماعيل حسين*

قسم الهندسة الكيمياوية، كلية الهندسة، جامعة بغداد، بغداد، العراق

الخلاصة

تتناول هذه الدراسة الخصائص المورفولوجية والأداء لغشاء الترشيح الفائق ذو الصفائح المسطحة الرقيقة؛ تم تقييم سلوك ترشيح صبغة الملكيت الأخضر (MG) في نظام الترشيح عبر التدفق. تضمنت الأغشية المحضرة دمج 16% بالوزن من البولي إيثر سلفون (PES) 0.5% بالوزن من البولي إيثيلين جلايكول 400 (PEG) عبر عملية عكس الطور. أدت إضافة PEG إلى تقليل استقطاب التركيز الداخلي، وتحسين محبة الغشاء للماء وتغيير أشكال المسام، مما يؤدي إلى تحسين أداء الغشاء. تم استخدام اختبارات SEM و AFM لتوصيف تكوين وبنية الغشاء. مع ظروف الصب المختلفة، تغير شكل الغشاء. تأثير سمك الغشاء (100، 150، 200) ميكرومتر وخواص حمام التخثر (درجة الحرارة (15، 25، 35) درجة مئوية وتركيب ,(30% 20, 10) DMF في الماء على المواد المصنعة لتقييم أداء الترشيح الغشائي، تم تطبيق الأغشية المصنعة في نظام الترشيح الفائق لمعالجة محلول صبغة الملكيت الأخضر عند تركيز (ppm 10) كملوث نموذجي، ووفقا للنتائج التي تم الحصول عليها، فإن الغشاء الأمثل من حيث السمك ودرجة الحرارة ومحتوى DMF هو (150) ميكرومتر، 35 درجة مئوية و10%DMF:Water على التوالي، وسجلت كفاءة الإزالة (94.5%، 93% و99.5%) على التوالي، في حين أن تدفق الماء كان (45، 35 و30) لتر/متر^2*ساعة.

الكلمات المفتاحية: غشاء UF المركب، خصائص الغشاء، إزالة الصبغة الخضراء، عملية تحول الطور، تدفق الماء.